International Journal of Computer Information Systems and Industrial Management Applications
ISSN 2150-7988 Volume 18(15s) 2026 pp. 41-53
https://doi.org/10.70917/ijcisim-2026-4346
Article

Reducing False-Negative Risk in Automated Pneumonia Screening Using Attention-Guided Deep Learning

Mohini Gahlot[1], Pinaki Ghosh[2]

[1]Department of *CSE*, Sage University Bhopal, INDIA
[2]Department of School of Advanced Computing Sage University Bhopal, INDIA
Email id: Mohinimoh425@gmail.com, Email id: pinaki.g@sageuniversity.edu.in

Abstract: .Pneumonia continues to be a major source of morbidity and mortality worldwide, especially in children, the elderly, and people with impaired immune systems. Due to its low cost and widespread availability, chest imaging radiology is the most often utilised diagnostic modality; yet, accurate interpretation is difficult and heavily dependent on radiologist expertise, which can result in clinically significant missed diagnosis. While deep learning-based methods have demonstrated potential for automated pneumonia detection, many of the models now in use rely on global feature learning, have poor interpretability, and do not adequately address the danger of false negatives. An attention-enhanced deep learning framework for clinically accurate pneumonia identification from chest imaging radiology is proposed in this study.To enhance spatial feature representation and highlight diagnostically significant lung regions, the framework combines a self-attention mechanism with a pretrained VGG16 backbone. To guarantee stable optimisation and efficient task adaptability, a two-stage training approach is used. The suggested model is tested using a single experimental methodology against many cutting-edge convolutional neural network architectures. The suggested framework obtains an accuracy of 96.3%, recall of 98.0%, F1-score of 97.5%, and ROC–AUC of 0.972, according to experimental results. Significantly, compared to the baseline VGG16 model, false-negative predictions are decreased from 27 to 17.
Keywords: Pneumonia Detection, Chest Imaging Radiology, Self-Attention Mechanism, Medical Image Analysis, False-Negative Reduction, and Convolutional Neural Networks (CNNs)

1. Introduction

Pneumonia is an acute pneumonia infection that is marked by inflammation and dysfunction of the alveols (Muhammad et al., 2021), the severity of which is usually dependent on age, as well as immunity (Stokes et al., 2021). It is still a serious international health issue leading to more than 450450 million new cases annually and high mortality (Kareem et al., 2022; Muhammad et al., 2021). Although chest imaging radiology is the most common diagnostic modality because it is easily available (Becker et al., 2022), it is usually limited by subtle distortions, thus making it difficult to interpret correctly. Other means, including lung sound analysis (Vidhya et al., 2022) are not as robust yet as it is necessary to roll out it in clinical practice. Recent developments of CNNs have shown to be more effective than the current classifiers in identifying pneumonia and COVID-19 (Alqudah et al., 2021; Yadav et al., 2024; Goyal and Singh, 2021; Ali et al., 2022; Zhang et al., 2020). Nevertheless, most representations are based on the global characteristics, which results in low spatial localization and high false-negative (Kareem et al., 2022). Moreover, standard assessments usually do not include such a crucial element of clinical safety as sensitivity (Stokes et al., 2021), and because these methods are black box, they do not give clinicians confidence. In order to counter such gaps, this paper hypothesizes an attention-directed framework. The model can localize diagnostically relevant areas to offer transparent and sensitive decision support to clinical screening by jointly training a self-attention mechanism with an existing backbone and employing activation mapping based on the gradient. The research gaps that are covered by the work, the objectives that are to be achieved, and the key contributions compared to the current pneumonia detecting approaches are summarized in Table 1.

Table 1. Alignment of Research Gap, Objectives, and Contributions

Research Gap	Research Objective	Key Contribution
Existing CNN-based pneumonia detection models lack explicit mechanisms to capture long-range spatial dependencies, resulting in suboptimal localization of pneumonia-related abnormalities in chest imaging radiology.	To design an attention-enhanced deep learning framework that improves spatial feature representation for pneumonia detection.	Proposes a self-attention–integrated CNN architecture that selectively emphasizes diagnostically relevant lung regions, improving spatial discrimination over conventional CNN models.
Most prior studies emphasize global metrics such as accuracy or ROC–AUC, while insufficiently addressing clinically critical outcomes such as false-negative predictions.	To reduce false-negative predictions in automated pneumonia screening.	Prioritizes recall and false-negative analysis, demonstrating improved clinical reliability compared to baseline architectures.
Explainability is often treated as a post-hoc visualization and is not systematically used to support diagnostic validation and clinical trust.	To incorporate explainability for transparent interpretation of model decisions.	Integrates Grad-CAM-based visual explanations to verify anatomically plausible attention regions, enhancing interpretability and clinician trust.

2. Related Work

Respiratory pandemics such as COVID-19 and pneumonia have triggered the global effect, thereby driving the research on automated diagnostic tools to aid in making clinical decisions. RT-PCR is still a standard, although due to its high cost and long turnaround times, its usage has been replaced by a chest radiograph that is accessible and has low radiation levels (Ibrahim et al., 2021; Jain et al., 2022; Becker et al., 2022; Dharmireddy et al., 2022).

In addition to imaging, non-imaging methods, such as electronic stethoscopes and cough analysis using AI, have been investigated (Vidhya et al., 2022; Alqudaihi et al., 2021). The techniques are however not always robust because of noise in the environment and fluctuation in patient cooperation. Therefore, it has turned into a field of machine learning and deep learning with respect to CXRs. Conventional methods that rely on the use of handcrafted characteristics, like SVM and the Random Forest, are promising and reach high scores, but tend to lack high generalization (Alqudah et al., 2021; Yahyaoui and Yumusak, 2021). On the other hand, other CNNs such as VGG16 and ResNet50 have also been shown to be highly successful when it comes to extracting features directly out of raw data (Yadav et al., 2024; Racic et al., 2021; Ali et al., 2022; Asnaoui et al., 2021; Sharma and Guleria, 2023).

With high accuracy rates, a number of gaps can be identified:

- Classification Scope: Numerous algorithms can be used to classify binary (e.g., COVID-19 vs. Normal), which is not as useful in differentiating between the viral, bacterial, and non-COVID pneumonia as an application in clinical workflows (Ibrahim et al., 2021).
- Complexity vs. Scalability: Hybrid architectures and multi-stage ensemble pipelines are also supposed to enhance performance but typically come with computational overhead and preprocessing complexity (Masad et al., 2021; Bhattacharyya et al., 2021; Ieracitano et al., 2022).
- Generalization: Most systems are not tested on a diverse and multicultural sample, especially in low- and middle-income areas (Togunwa et al., 2025).
- Interpretability Deep learning is black-box, which prevents clinical trust (Kaplan et al., 2021; Boddu et al., 2021).

Existing studies emphasize that algorithms that combine explainability and enhance spatial localization of abnormalities as well as prioritize diagnostic sensitivity to minimize false negative should be developed. This research fills these gaps by coming up with a valid, explicable diagnostic model..

3. Research Methodology

The proposed system is a two-step interpretable deep learning framework that aims at automated pneumonia classification in the chest imaging radiology images. The architecture incorporates a VGG16 backbone, a self-attention module, and a Grad-CAM explainable module. The overall architecture of the designed system, shown in Figure 1, is a two-stage architecture, comprising of a pretrained convolutional backbone, self-attention mechanism, and a probabilistic classification head that enables accurate, reliable and explainable diagnostic predictions.

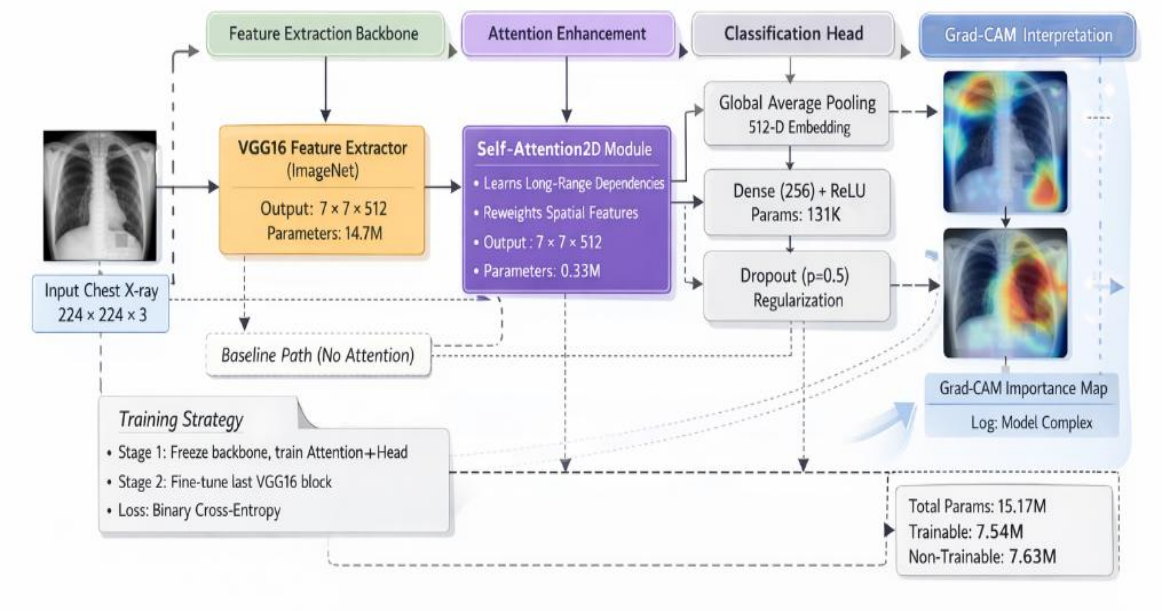

Fig 1. Proposed VGG16 With Self-Attention Architecture For Pneumonia Detection

Let $\mathcal{D} = \{(x_i, y_i)\}_{i=1}^{N}$ be the labeled dataset where $x_i \in \mathbb{R}^{H\times W\times 3}$ is the input image and $y_i \in \{0,1\}$ is the class label (0: normal, 1: pneumonia). The framework learns a mapping function:

$$f_\theta: \mathbb{R}^{H\times W\times 3} \to [0,1] \quad (1)$$

The predicted probability is defined as$\hat{y}_i = f_\theta(x_i)$.

Feature Extraction: A convolutional extractor $\phi(\cdot)$ generates a feature tensor:

$$F_i = \phi(x_i) \in \mathbb{R}^{h\times w\times c} \quad (2)$$

Spatial Attention: A learned spatial map $\alpha_i \in \mathbb{R}^{h\times w}$ refines the features via element-wise multiplication:

$$F_i' = \alpha_i \odot F_i \quad (3)$$

Classification: Using Global Average Pooling (GAP) and a Sigmoid activation function:

$$z_i = \mathrm{GAP}(F_i') \in \mathbb{R}^c \quad (4)$$

$$\hat{y}_i = \sigma(W z_i + b) \quad (5)$$

3.1 Dataset Description

The study utilizes the Kermany et al. (2018) dataset from Kaggle. It consists of frontal radiographs categorized into "Normal" and "Pneumonia" classes.

Table 2. Class-wise distribution of the chest imaging radiology dataset

Class	Training Samples	Test Samples	Total Samples
Normal	1,108	317	1,425
Pneumonia	2,991	855	3,846

Total	**4,099**	**1,172**	**5,271**

The bias in the data regarding the class imbalance is representative of the situation in the clinical screening, where pneumonia cases are often over-represented as a result of symptom-based imaging procedures. The dataset is chosen because it was widely used in previous pneumonia detection, and thus, comparisons can be reproducible, and its binary classification environment, which directly corresponds to the real-world goals in screening.

3.2 Data Preprocessing

Images are standardized to ensure compatibility with the VGG16 architecture.

- Spatial Scaling: Images are resized to 224×224 pixels.
- Channel Replication: Grayscale images $x_i \in \mathbb{R}^{H\times W}$ are converted to three-channel tensors:

$$x_i^{(3)} = \text{Replicate}(x_i) \in \mathbb{R}^{224\times 224\times 3} \tag{6}$$

- Intensity Normalization: Pixel values $x_{i,p}$ are scaled using the pretraining mean (μ) and standard deviation (σ):

$$\tilde{x}_{i,p} = \frac{x_{i,p}-\mu}{\sigma} \tag{7}$$

3.3 Training and Optimization

The dataset is partitioned into disjoint sets:

$$\mathcal{D} = \mathcal{D}_{\text{train}} \cup \mathcal{D}_{\text{val}} \cup \mathcal{D}_{\text{test}}, \mathcal{D}_{\text{train}} \cap \mathcal{D}_{\text{test}} = \emptyset \tag{8}$$

To address class imbalance, class-weighted loss is implemented. For n_c samples in class $c \in \{0,1\}$ and total samples N, the weights w_c are:

$$w_c = \frac{N}{2n_c}, c \in \{0,1\} \tag{9}$$

Optimization: Weights are applied to the loss function to increase sensitivity toward the minority class.

Augmentation Policy: Aggressive geometric transformations are avoided to preserve the clinical integrity of the anatomical structures.

3.4 Proposed Architecture

The anticipated architecture integrates a convolutional backbone with an attention-driven spatial refinement mechanism to identify pneumonia from chest imaging radiology. This design balances diagnostic performance, interpretability via Grad-CAM, and computational efficiency.

3.4.1 Backbone Network for Hierarchical Feature Extraction

A pretrained VGG16 network serves as the backbone for hierarchical feature extraction. Given a processed input image:

$$\tilde{x}_i \in \mathbb{R}^{224\times 224\times 3} \tag{10}$$

The backbone applies successive convolutional and max-pooling operations to extract a high-level feature tensor:

$$F_i = \phi(\tilde{x}_i) \in \mathbb{R}^{7\times 7\times 512} \tag{11}$$

where $\phi(\cdot)$denotes the nonlinear mapping learned during ImageNet pretraining. VGG16 is selected for its stable gradient propagation and spatial resolution suitable for subsequent attention refinement.

3.4.2 Self-Attention Module for Spatial Feature Refinement

To capture long-range spatial dependencies often missed by standard convolutional layers, a self-attention module is positioned after the backbone.Figure 2. shows the example of end-to-end architecture, which is made of

pretrained VGG16 backbone (hierarchical feature extraction), self-attention module (spatial feature refinement), and a lightweight classification head. The attention mechanism highlights pneumonia-relevant lungs areas, whereas the Grad-CAM output is visual interpretation as it highlights areas that contribute the most to the final prediction.

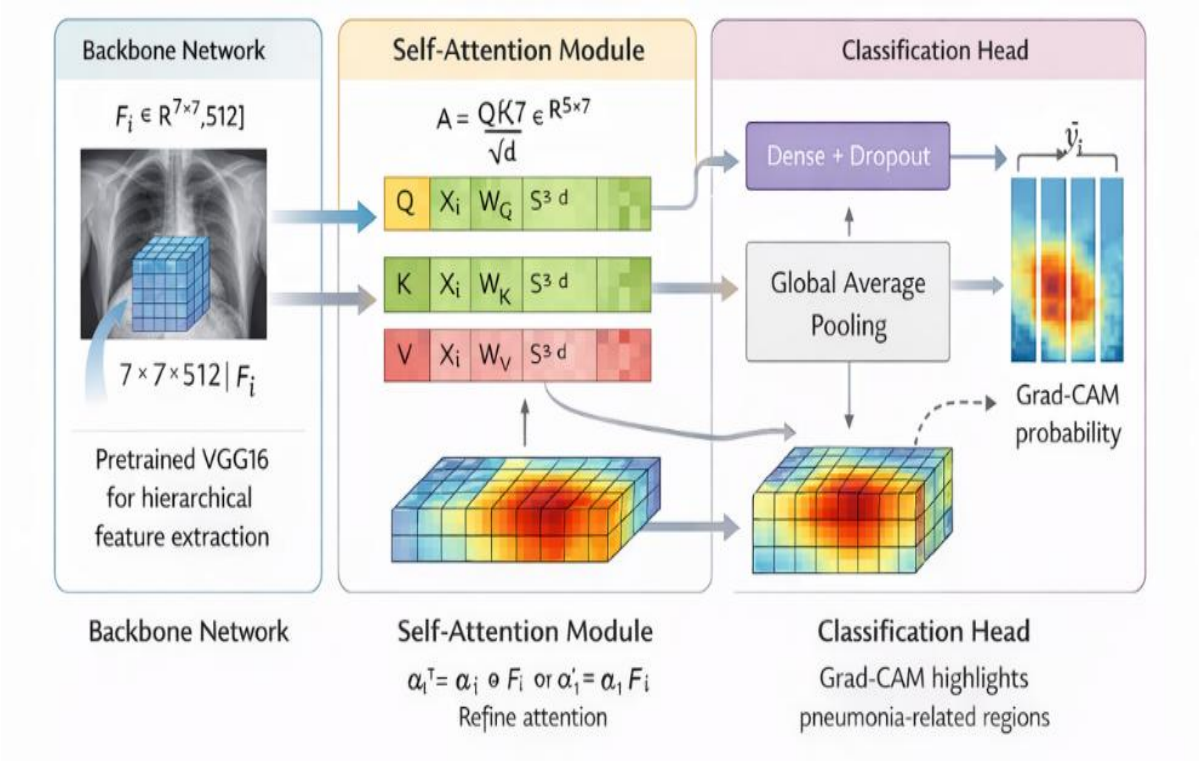

Fig.2. Attention-based pneumonia detection system

Let the channel-wise feature maps be represented as:

$$F_i = [f_i^{(1)}, f_i^{(2)}, \dots, f_i^{(c)}] \tag{12}$$

where $c = 512$, The module learns a spatial attention map.

$$\alpha_i \in \mathbb{R}^{7\times7} \tag{13}$$

The refined feature representation F_i' is calculated via element-wise multiplication across all channels:

$$F_i' = \alpha_i \odot F_i \tag{14}$$

This mechanism emphasizes pneumonia-relevant regions (e.g., opacities, consolidations) while suppressing background noise and irrelevant anatomical structures.

3.4.3 Global Feature Aggregation, Classification, and Architectural Design

The refined tensor $Fi' \in \mathbb{R}^{7\times7\times512}$ is aggregated using Global Average Pooling (GAP) to reduce dimensionality while preserving semantic information:

$$z_i = \frac{1}{hw}\sum_{u=1}^{h}\sum_{v=1}^{w} F_i'(u,v) \tag{15}$$

where $h = w = 7$, resulting in a vector $z_i \in \mathbb{R}^{512}$. The classification head processes this vector to produce the final prediction:

$$\hat{y}_i = \sigma(W_2(\mathrm{ReLU}(W_1 z_i + b_1)) + b_2) \tag{16}$$

where W_1, W_2 and b_1, b_2 denote trainable parameters, and $\sigma(\cdot)$ represents the sigmoid activation function. The most important architectural components as well as their output dimensions and the numbers of their parameters are

summarized in Table 3. Although the layers like the global average pooling, dropout, and activation functions do not add to the trainable parameters, they are essential to feature aggregation, regularization and stability of the model.

Table 3. Architectural components of the proposed VGG16–Self-Attention model

Module	Layer Type	Output Shape	Parameters
Input	Chest Imaging Radiology		0
Backbone	VGG16 Conv Blocks		14,714,688
Attention	Self-Attention2D		328,321
Pooling	Global Average Pooling	512	0
Classifier	Dense (256) + ReLU	256	131,328
Regularization	Dropout	256	0
Output	Dense (Sigmoid)	1	257
Total	—	—	**15,174,594**

The modularity of this design allows the self-attention component to be integrated with alternative backbones in future iterations without requiring a full architectural redesign.

3.5 Training Strategy and Optimization

The proposed framework training plan is well-crafted so that the convergence will be stable, there will be no overfitting, and the previously trained knowledge will be retained, and the framework could be effectively adapted to the specific task. Medical imaging data, especially the chest imaging radiology data, is typically small in size and has a class imbalance, which leads to unstable gradient and catastrophic forgetting with naive end-to-end training. A two stage optimization strategy is used to solve these issues and this is represented in Figure 3.

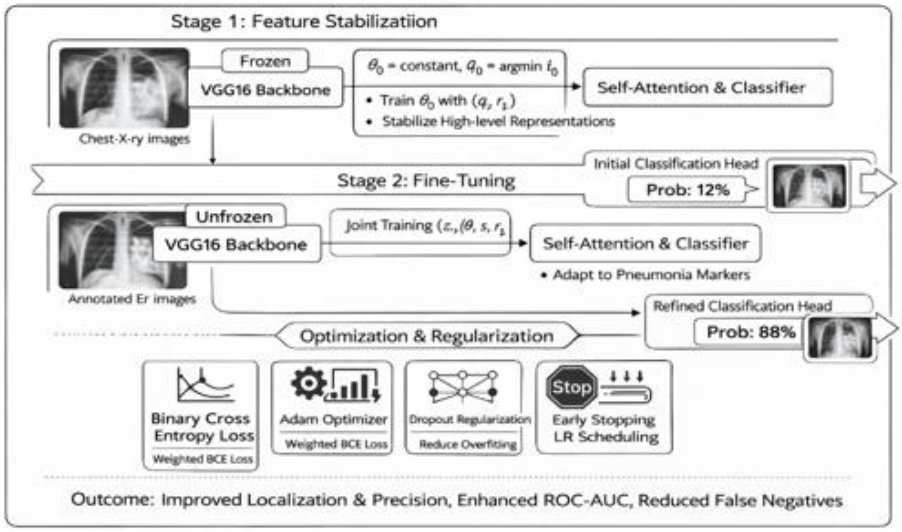

Figure 3. Two-stage training strategy and optimization framework for pneumonia detection.

To address class imbalance and gradient instability in medical imaging, a two-stage optimization strategy is employed. This approach prevents catastrophic forgetting and ensures stable convergence by separating feature stabilization from domain-specific refinement.

1. Stage 1: Feature Stabilization

The convolutional layers of the VGG16 backbone are frozen to preserve generic spatial hierarchies. Only the self-attention module and classification head are trained.

$$\theta_b = \text{constant}, \theta_h \leftarrow \arg\min_{\theta_h} \mathcal{L} \qquad (17)$$

where θ_b represents backbone parameters and θ_h represents the attention and head parameters.

2. Stage 2: Fine-Tuning

The final convolutional block is unfrozen and trained alongside the classification subunits using a significantly lower learning rateη to adapt to pneumonia-specific radiographic patterns.

$$\theta_b^*, \theta_h^* \leftarrow \arg\min_{\theta_b, \theta_h} \mathcal{L} \text{with} \eta \ll \eta_{\text{Stage 1}} \qquad (18)$$

3. Loss Function and Hyperparameters

The model is optimized using Binary Cross-Entropy (BCE) loss:

$$\mathcal{L}_{\text{BCE}} = -\frac{1}{N}\sum_{i=1}^{N}[y_i \log(\hat{y}_i) + (1 - y_i)\log(1 - \hat{y}_i)] \quad (19)$$

- Optimizer: Adam ($\eta = 1 \times 10^{-4}, \eta = 1 \times 10^{-5}$).
- Regularization: Dropout, Early Stopping, and Learning Rate Scheduling.

3.6 Evaluation Metrics

The framework is evaluated using metrics derived from the Confusion Matrix to ensure clinical reliability.The projected pneumonia detection model is tested against several measures to guarantee the quality of diagnostic and clinical reliability of the model which are presented in Table 4 along with its interpretation by the clinical meaning.

Table 4. Evaluation metrics with mathematical formulations and clinical relevance

Metric	Mathematical Formulation	Clinical Interpretation
Confusion Matrix	TP, TN, FP, FN	Provides case-level outcomes; FN represents missed pneumonia cases, which are clinically critical
Accuracy	$\frac{TP + TN}{TP + TN + FP + FN}$	Assesses overall accuracy but may obscure inadequate pneumonia identification in skewed datasets
Precision	$\frac{TP}{TP+FP}$	Demonstrates the dependability of pneumonia-positive forecasts; crucial for minimizing superfluous follow-up
Recall (Sensitivity)	$\frac{TP}{TP+FN}$	Measures the ability to detect pneumonia cases; prioritized to minimize missed diagnoses
F1-score	$2 \cdot \frac{\text{Precision} \cdot \text{Recall}}{\text{Precision} + \text{Recall}}$	Balances detection performance and false alarms in clinical screening
ROC–AUC	$\int_0^1 \text{TPR}(t)\, d(\text{FPR}(t))$	Evaluates discriminative capability independent of decision threshold

3.7 Explainability Using Grad-CAM

To present graphical substantiation for clinical determinations, Grad-CAM evaluates the significance of each neuron by assessing the gradient of the score for class (y^c) in relation to feature map activations A^k:

$$\alpha_k^c = \frac{1}{Z}\sum_i \sum_j \frac{\partial y^c}{\partial A_{ij}^k} \qquad (20)$$

Where Z is the spatial normalizing coefficient. The final derived heatmap is produced by a weighted linear amalgamation succeeded by a ReLU activating.:

$$L^{c}_{\text{Grad-CAM}} = \text{ReLU}\left(\sum_{k} \alpha^{c}_{k} A^{k}\right) \quad (21)$$

This localization ensures the model focuses on opacities and consolidations rather than anatomical background.

4.Result Analysis

4.1 Experimental Setup and Test Protocol

To facilitate a balanced and reproducible comparison, all the models (VGG16, DenseNet121, ResNet50, EfficientNetB0 and the proposed architecture) were compared on a standard protocol and under the same data division and a fixed decision threshold of 0.5. The test set, which is summarized in Table 5, represents a clinical imbalance which is realistic, consisting of 855 cases of pneumonia and 317 normal cases (1,172 cases in total). With this distribution, recall and precision-recall analysis with accuracy was evaluated initially. According to Fig. 4, subtle variations between the clear lung fields in normal scans and the opacities or consolidations of pneumonia cases present the classification task and make the model focus on localized and clinically significant features.

Table 5. Test dataset composition used for performance evaluation

Class	**Number of Samples**
NORMAL	317
PNEUMONIA	855
Total	**1172**

To provide consistent and fair comparisons of performance between different models, all models were tested under the same experimental protocol, i.e. including VGG16, DenseNet121, ResNet50, EfficientNetB0 and the proposed attention-enhanced VGG16.

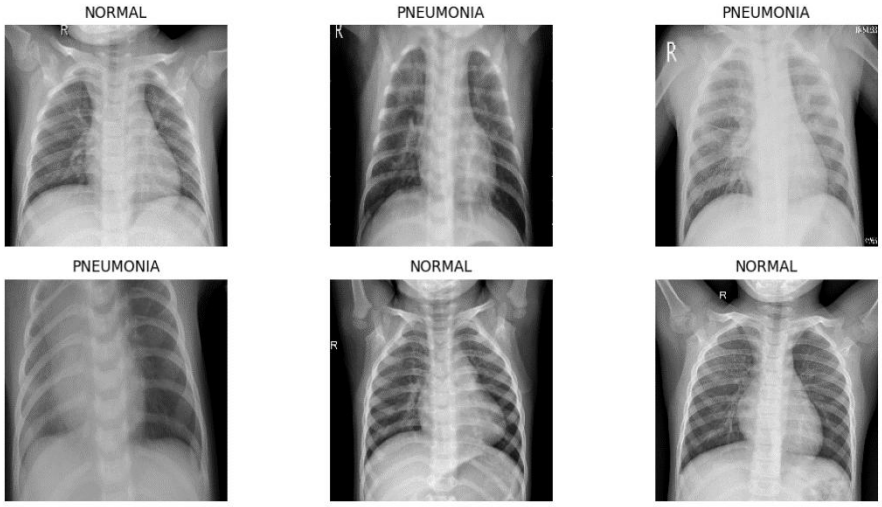

Fig.4. Representative chest imaging radiology from the test dataset illustrating normal and pneumonia cases

4.2 Quantitative Performance Comparison Across Models

Table 6 is a summary of a quantitative comparison between the proposed attention-enhanced model and the baseline and state-of-the-art CNN architectures through conventional classification metrics. The VGG16 proposed with self-attention is the best-balanced performance, as it has the highest recall and F1-score, which means that it is much more sensitive to pneumonia cases, although its accuracy and precision are quite high. The results, as compared to the baseline VGG16 and more profound designs like ResNet50 and EfficientNetB0, indicate that the addition of attention-guided spatial refinement enhances diagnostic sensitivity yet does not reduce precision, which makes the framework more dependable in terms of clinical screening.

Table 6. Comparative Performance Metrics of Different Models

Model	Accuracy	Precision	Recall	F1-score	AUC
DenseNet121	0.940	0.964	0.953	0.959	0.976
Proposed (VGG16 + Attention)	**0.963**	**0.970**	**0.980**	**0.975**	0.972
VGG16	0.951	0.965	0.968	0.967	0.942
ResNet50	0.875	0.930	0.897	0.913	0.935
EfficientNetB0	0.712	0.797	0.812	0.804	0.703

4.3 Error Analysis and Clinical Risk Assessment

To examine the clinical risks of pneumonia screening in terms of false positives and false negatives, Table 7 provides the error level analysis. The VGG16 with self-attention proposed has the least number of false-negatives and the model reduces the missed cases of pneumonia significantly when compared to VGG16 and more complex architectures like ResNet50 and EfficientNetB0. This decrease shows that attention-directed spatial refinement enhances the ability to detect minor pneumonia patterns, and the framework overall is more appropriate in real-world screening scenarios in which reducing false negative outcomes is a crucial goal.

Table 7. Error Profile Comparison of Different Models

Model	False Positives	False Negatives
DenseNet121	30	40
Proposed (VGG16 + Attention)	**26**	**17**
VGG16	30	27
ResNet50	58	88
EfficientNetB0	177	161

4.4 ROC Curve Analysis

Figure 5 demonstrates the receiver operating characteristic curves of all considered models, which indicate that they have threshold-free discriminative performance on the test set. The proposed VGG16 with self attention can reach a high AUC of 0.972 and has a steeper initial ROC slope, meaning that it is more sensitive at low false-positive rates, and this property is especially attractive when screening is required by clinics.

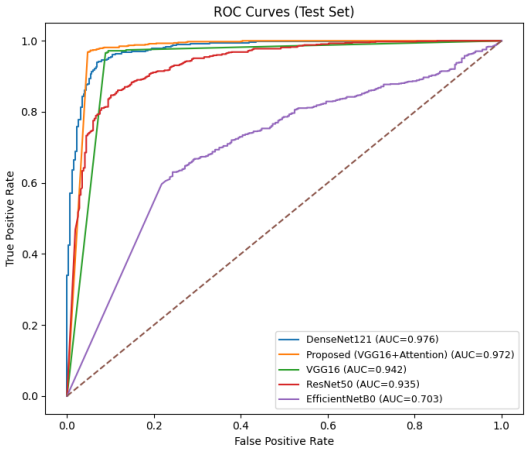

Fig.5. ROC curves highlighting improved sensitivity of the proposed model for pneumonia detection

4.5 Precision–Recall Curve Analysis

Figure 6 shows the precision-recall curves of all the tested models and this provides a performance evaluation in case of class imbalance. The suggested VGG16 with self-attention has high accuracy with the large range of recall values, meaning that the high sensitivity is attained without the equivalent growth in false-positive predictions, which is preferable in clinical screening of pneumonia.

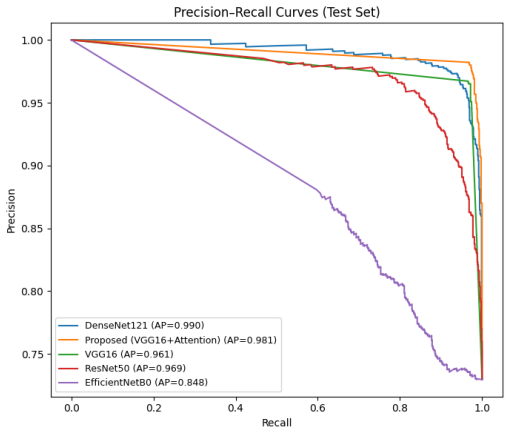

Fig.6. Precision–recall curves of evaluated models on the test set under class imbalance.

The suggested architecture exhibits a better precision-recall trade-off than more profound models. Although EfficientNetB0 suffers a severe accuracy decline when recall is high, and DenseNet121 demonstrates competitive stability with a lower error, our model does not lose its high accuracy as sensitivity grows. This tradeoff is essential to clinical screening, in which reducing false-negatives should not lead to a load of diagnosis. The precision-recall analysis also confirms that the model is not easily affected by imbalanced data, which proves its usefulness in real-life pneumonia triage.

4.6 Explainability and Grad-CAM-Based Visual Analysis

Grad-CAM was applied to see the steps taken by the model in order to instill trust in clinical decision-making. As explained in Fig. 7, the pneumonia cases in heatmap always show an anatomically pertinent region, including opacities, and infiltrates. Normal cases on the other hand demonstrate diffuse minimal activation. This correspondence between the spatial orientation of the model and the identified radiographic phenotypes makes it clear that the predictions are not made based on artifacts but rather on clinically plausible evidence, which makes the framework a clear and reliable tool of decision-making.

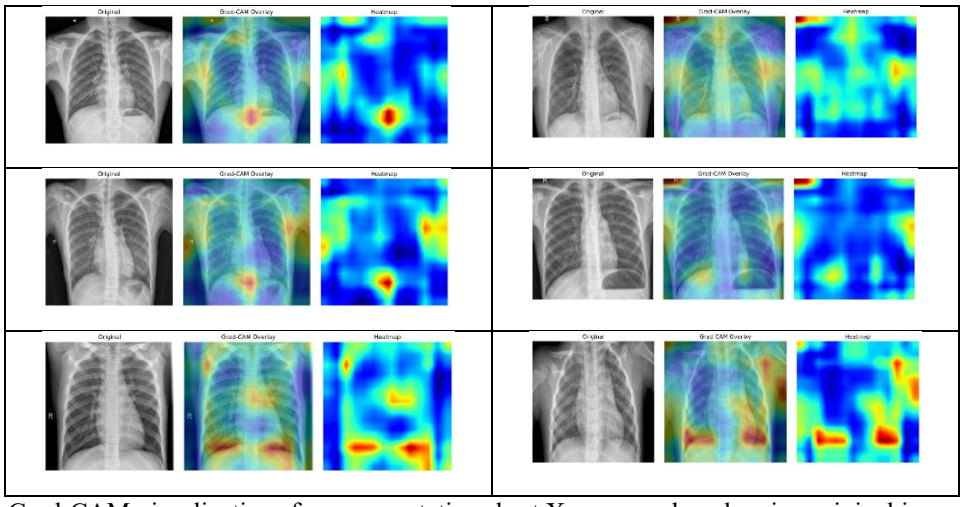

Fig.7. Grad-CAM visualizations for representative chest X-ray samples, showing original images, heatmaps, and overlays for pneumonia and normal cases

The analysis with the use of Grad-CAM proves that the suggested model is efficient with respect to quantitative considerations and employs clinically acceptable visual data to arrive at conclusions. The correlation between the focus of the model and the recognized chest imaging radiology signs of pneumonia adds to the trustworthiness and possible acceptance of the suggested model as decision support tool.

5. Discussion

The main aim of this paper is to present how the findings of the study may be used to achieve three main goals. These three goals include the presentation of spatial information, the reduction of false negatives, and the ability to explain the results of the study.

1. Enhancement of Spatial Feature Representation

By introducing the self-attention steps into the CNN design, it was able to increase the ability to detect localized affected signatures. The conclusion indicate that attention-based spatial refinement proves to be more efficient to detect pneumonia than just deepening a network (e.g., VGG16). The framework demonstrated higher F1-scores by putting more emphasis on diagnostically relevant pixels than global noise as evidence that the framework had learned a more complex representation of lung anatomy and disease patterns.

2. Mitigation of False-Negatives in Automated Screening

The framework was optimized to reduce the number of missed diagnoses to achieve the goal of clinical safety. The model showed a large decrease in the false-negative predictions, in terms of high recall and ROC-AUC values. Automated triage would highly rely on this performance profile; by not letting the finer instances of pneumonia slip by, the model would be consistent with the high stakes needs of clinical screening where sensitivity is the most important consideration.

3. Transparency through Model Explainability

The purpose of opaque interpretation was met by applying the Grad-CAM visual validation. This architecture contrasted with the more traditional "black-box" CNNs by generating localised sharp attention maps, which are associated with anatomically plausible objects, including opacities and consolidations. This direct connection between internal weights of the model and clinical pathology gives the explainability needed to build trust in the physicians and enable the adoption of AI in the diagnostic processes.

4. Clinical Implications and Future Directions

The findings support the notion that learning focusing on specific information is successful in closing the gap between raw quantitative performance and therapeutic benefits. Although the model is highly accurate and safe, the following limitations will still be addressed:

- Generalization: The verification of the framework on multiple datasets in order to ensure the stability of performance across different types of images is the generalization.
- Expansion: Extending the architecture to multi-class thoracic disease classification.
- Integration: Incorporating clinical priors (e.g., patient history) directly into the attention mechanism to further refine diagnostic precision.

The framework that has been constructed serves to accomplish the goals of the study by linking high-performance deep learning to the clinical foundations of spatial precision, safety of diagnosis, and interpretability.

6. Conclusion

In this work, the authors used a fully automated attention mechanism with a pre-trained VGG16 that is aimed at developing an attention-perceptive deep learning algorithms for the identification of pneumonia based on the data of chest imaging radiology. The goal of the system is to increase spatial discrimination of features and sensitivity to the anomalies associated with pneumonia. The results of the paper show that the system achieves 96.3% accuracy, 98.0% recall, 97.5% F-beta value, as well as 0.9720 ROC-AUC result, which are higher than the values obtained for the earlier VGG16 and different other deep systems based on clinically important measures. In particular, it is important to note that the model provides proper improvement of the screening safety decreasing the number of false-negative results from 2727 to 1717 in comparison with the baseline. Moreover, the precision-recall and ROC studies provide evidence that the model performs effectively irrespective of the class imbalance. In addition, the visual explanations obtained using Grad-CAM show that the model works very well in areas where lungs have a proper

physiology. This improves the interpretability of the model and clinical confidence necessary for successful practical implementation. Thus, the study proves that the guided attention spatial optimization works much better than just making the networks deeper.

Reference

1. Ali, A. M., Ghafoor, K., Mulahuwaish, A., & Maghdid, H. (2022). COVID-19 pneumonia level detection using deep learning algorithm and transfer learning. Evolutionary Intelligence, 17(2), 1035–1046. https://doi.org/10.1007/s12065-022-00777-0
2. Alqudah, A. M., Qazan, S., & Masad, I. S. (2021). Artificial Intelligence Framework for Efficient detection and Classification of pneumonia using chest radiography images. Journal of Medical and Biological Engineering. https://doi.org/10.1007/s40846-021-00631-1
3. Alqudaihi, K. S., Aslam, N., Khan, I. U., Almuhaideb, A. M., Alsunaidi, S. J., Ibrahim, N. M. a. R., Alhaidari, F. A., Shaikh, F. S., Alsenbel, Y. M., Alalharith, D. M., Alharthi, H. M., Alghamdi, W. M., & Alshahrani, M. S. (2021). Cough sound detection and diagnosis using Artificial Intelligence Techniques: Challenges and opportunities. IEEE Access, 9, 102327–102344. https://doi.org/10.1109/access.2021.3097559
4. Asnaoui, K. E., Chawki, Y., & Idri, A. (2021). Automated methods for detection and classification pneumonia based on X-Ray images using deep learning. In Studies in big data (pp. 257–284). https://doi.org/10.1007/978-3-030-74575-2_14
5. Barakat, N., Awad, M., & Abu-Nabah, B. A. (2023). A machine learning approach on chest X-rays for pediatric pneumonia detection. Digital Health, 9, 20552076231180008. https://doi.org/10.1177/20552076231180008
6. Becker, J., Decker, J. A., Römmele, C., Kahn, M., Messmann, H., Wehler, M., Schwarz, F., Kroencke, T., & Scheurig-Muenkler, C. (2022). Artificial Intelligence-Based detection of pneumonia in chest radiographs. Diagnostics, 12(6), 1465. https://doi.org/10.3390/diagnostics12061465
7. Bhattacharyya, A., Bhaik, D., Kumar, S., Thakur, P., Sharma, R., & Pachori, R. B. (2021). A deep learning based approach for automatic detection of COVID-19 cases using chest X-ray images. Biomedical Signal Processing and Control, 71, 103182. https://doi.org/10.1016/j.bspc.2021.103182
8. Boddu, R. S. K., Karmakar, P., Bhaumik, A., Nassa, V. K., Vandana, & Bhattacharya, S. (2021). Analyzing the impact of machine learning and artificial intelligence and its effect on management of lung cancer detection in covid-19 pandemic. Materials Today Proceedings, 56, 2213–2216. https://doi.org/10.1016/j.matpr.2021.11.549
9. Chiwariro, R., & Wosowei, J. B. (2023). Comparative Analysis of Deep Learning Convolutional Neural Networks based on Transfer Learning for Pneumonia Detection. International Journal for Research in Applied Science and Engineering Technology, 11(1), 1161–1170. https://doi.org/10.22214/ijraset.2023.48685
10. Dharmireddy, A., Manohar, A. S., Hari, G., Gayatri, G., Venkateswarlu, A., & Sai, C. T. (2022). Detection of COVID-19 from X-RAY Images using Artificial Intelligence (AI). 2022 2nd International Conference on Intelligent Technologies (CONIT), 1–5. https://doi.org/10.1109/conit55038.2022.9847741
11. Goyal, S., & Singh, R. (2021). Detection and classification of lung diseases for pneumonia and Covid-19 using machine and deep learning techniques. Journal of Ambient Intelligence and Humanized Computing, 14(4), 3239–3259. https://doi.org/10.1007/s12652-021-03464-7
12. Ibrahim, A. U., Ozsoz, M., Serte, S., Al-Turjman, F., & Yakoi, P. S. (2021). Pneumonia Classification Using Deep Learning from Chest X-ray Images During COVID-19. Cognitive Computation, 16(4), 1589–1601. https://doi.org/10.1007/s12559-020-09787-5
13. Ieracitano, C., Mammone, N., Versaci, M., Varone, G., Ali, A., Armentano, A., Calabrese, G., Ferrarelli, A., Turano, L., Tebala, C., Hussain, Z., Sheikh, Z., Sheikh, A., Sceni, G., Hussain, A., & Morabito, F. C. (2022). A fuzzy-enhanced deep learning approach for early detection of Covid-19 pneumonia from portable chest X-ray images. Neurocomputing, 481, 202–215. https://doi.org/10.1016/j.neucom.2022.01.055
14. Islam, R., & Tarique, M. (2022). Chest X-Ray Images to Differentiate COVID-19 from Pneumonia with Artificial Intelligence Techniques. International Journal of Biomedical Imaging, 2022, 1–15. https://doi.org/10.1155/2022/5318447
15. Jain, D. K., Singh, T., Saurabh, P., Bisen, D., Sahu, N., Mishra, J., & Rahman, H. (2022). Deep Learning-Aided Automated Pneumonia detection and classification using CXR scans. Computational Intelligence and Neuroscience, 2022, 1–19. https://doi.org/10.1155/2022/7474304
16. Kaplan, A., Cao, H., FitzGerald, J. M., Iannotti, N., Yang, E., Kocks, J. W., Kostikas, K., Price, D., Reddel, H. K., Tsiligianni, I., Vogelmeier, C. F., Pfister, P., & Mastoridis, P. (2021). Artificial Intelligence/Machine Learning in Respiratory Medicine and potential role in asthma and COPD diagnosis. The Journal of Allergy and Clinical Immunology in Practice, 9(6), 2255–2261. https://doi.org/10.1016/j.jaip.2021.02.014
17. Kareem, A., Liu, H., & Sant, P. (2022). Review on Pneumonia Image Detection: A Machine Learning Approach. Human-Centric Intelligent Systems, 2(1–2), 31–43. https://doi.org/10.1007/s44230-022-00002-2
18. Kermany, D. S., Goldbaum, M., Cai, W., Valentim, C. C. S., Liang, H., Baxter, S. L., et al. (2018). Identifying medical diagnoses and treatable diseases by image-based deep learning. *Cell, 172*(5), 1122–1131.e9. https://doi.org/10.1016/j.cell.2018.02.010
19. Kwon, T., Lee, S. P., Kim, D., Jang, J., Lee, M., Kang, S. U., Kim, H., Oh, K., On, J., Kim, Y. J., Yun, S. J., Jin, K. N., Kim, E. Y., & Kim, K. G. (2021). Diagnostic performance of artificial intelligence model for pneumonia from chest radiography. PLoS ONE, 16(4), e0249399. https://doi.org/10.1371/journal.pone.0249399

20. Masad, I. S., Alqudah, A., Alqudah, A. M., & Almashaqbeh, S. (2021). A hybrid deep learning approach towards building an intelligent system for pneumonia detection in chest X-ray images. International Journal of Power Electronics and Drive Systems/International Journal of Electrical and Computer Engineering, 11(6), 5530. https://doi.org/10.11591/ijece.v11i6.pp5530-5540
21. Muhammad, Y., Alshehri, M. D., Alenazy, W. M., Hoang, T. V., & Alturki, R. (2021). Identification of pneumonia disease applying an intelligent computational framework based on deep learning and machine learning techniques. Mobile Information Systems, 2021, 1–20. https://doi.org/10.1155/2021/9989237
22. Racic, L., Popovic, T., Cakic, S., & Sandi, S. (2021). Pneumonia Detection Using Deep Learning Based on Convolutional Neural Network. International Conference on Information Technology (IT), 1–4. https://doi.org/10.1109/it51528.2021.9390137
23. Sharma, S., & Guleria, K. (2023). A Deep Learning based model for the Detection of Pneumonia from Chest X-Ray Images using VGG-16 and Neural Networks. Procedia Computer Science, 218, 357–366. https://doi.org/10.1016/j.procs.2023.01.018
24. Stokes, K., Castaldo, R., Federici, C., Pagliara, S., Maccaro, A., Cappuccio, F., Fico, G., Salvatore, M., Franzese, M., & Pecchia, L. (2021). The use of artificial intelligence systems in diagnosis of pneumonia via signs and symptoms: A systematic review. Biomedical Signal Processing and Control, 72, 103325. https://doi.org/10.1016/j.bspc.2021.103325
25. Szepesi, P., & Szilágyi, L. (2022). Detection of pneumonia using convolutional neural networks and deep learning. Journal of Applied Biomedicine, 42(3), 1012–1022. https://doi.org/10.1016/j.bbe.2022.08.001
26. Togunwa, T. O., Babatunde, A. O., Fatade, O. E., Olatunji, R., Ogbole, G., & Falade, A. (2025). Detection of pneumonia in children through chest radiographs using artificial intelligence in a low-resource setting: A pilot study. PLOS Digital Health, 4(9), e0000713. https://doi.org/10.1371/journal.pdig.0000713
27. Vidhya, B., Madhav, M. N., Kumar, M. S., & Kalanandini, S. (2022). AI based diagnosis of pneumonia. Wireless Personal Communications, 126(4), 3677–3692. https://doi.org/10.1007/s11277-022-09885-7
28. Yadav, S., Rizvi, S. a. M., & Agarwal, P. (2024). Detection of Lung Diseases for Pneumonia, Tuberculosis, and COVID-19 with Artificial Intelligence Tools. SN Computer Science, 5(3). https://doi.org/10.1007/s42979-024-02617-7
29. Yahyaoui, A., & Yumusak, N. (2021). Deep and machine learning towards pneumonia and asthma detection. 2021 International Conference on Innovation and Intelligence for Informatics, Computing, and Technologies (3ICT), 494–497. https://doi.org/10.1109/3ict53449.2021.9581963
30. Yi, R., Tang, L., Tian, Y., Liu, J., & Wu, Z. (2021). Identification and classification of pneumonia disease using a deep learning-based intelligent computational framework. Neural Computing and Applications, 35(20), 14473–14486. https://doi.org/10.1007/s00521-021-06102-7
31. Zhang, R., Tie, X., Qi, Z., Bevins, N. B., Zhang, C., Griner, D., Song, T. K., Nadig, J. D., Schiebler, M. L., Garrett, J. W., Li, K., Reeder, S. B., & Chen, G. (2020). Diagnosis of Coronavirus Disease 2019 Pneumonia by Using Chest Radiography: Value of Artificial Intelligence. Radiology, 298(2), E88–E97. https://doi.org/10.1148/radiol.2020202944